Infrastructure assisted adaptive driving to stabilise heterogeneous vehicle strings

Wang, Meng

DOI
10.1016/j.trc.2018.04.010

Publication date
2018

Document Version
Accepted author manuscript

Published in
Transportation Research Part C: Emerging Technologies

Citation (APA)
Wang, M. (2018). Infrastructure assisted adaptive driving to stabilise heterogeneous vehicle strings. *Transportation Research Part C: Emerging Technologies*, *91*, 276-295. https://doi.org/10.1016/j.trc.2018.04.010

Infrastructure Assisted Adaptive Driving to Stabilise Heterogeneous Vehicle Strings *

Meng Wang

Department of Transport & Planning, Delft University of Technology, the Netherlands
m.wang@tudelft.nl

Abstract

Literature has shown potentials of Connected/Cooperative Automated Vehicles (CAVs) in improving highway operations, especially on roadway capacity and flow stability. However, benefits were also shown to be negligible at low market penetration rates. This work develops a novel adaptive driving strategy for CAVs to stabilise heterogeneous vehicle strings by controlling one CAV under vehicle-to-infrastructure (V2I) communications. Assumed is a roadside system with V2I communications, which receives control parameters of the CAV in the string and estimates parameters *imperfectly* of non-connected automated vehicles. It determines the adaptive control parameters (e.g. desired time gap and feedback gains) of the CAV if a downstream disturbance is identified and sends them to the CAV. The CAV changes its behaviour based on the adaptive parameters *commanded* by the roadside system to suppress the disturbance.

The proposed adaptive driving strategy is based on string stability analysis of heterogeneous vehicle strings. To this end, linearised vehicle dynamics model and control law are used in the controller parametrisation and Laplace transform of the speed and gap error dynamics in time domain to frequency domain enables the determination of sufficient string stability criteria of heterogeneous strings. The analytical string stability conditions give new insights into automated vehicular string stability properties in relation to the system properties of time delays and controller design parameters of feedback gains and desired time gap. It further allows the quantification of a *stability margin*, which is subsequently used to adapt the feedback control gains and desired time gap of the CAV to suppress the amplification of gap and speed errors through the string.

Analytical results are verified via systematic simulation of both homogeneous and heterogeneous strings. Simulation demonstrates the predictive power of the analytical string stability conditions. The performance of the adaptive driving strategy under V2I cooperation is tested in simulation. Results show that even the estimation of control parameters of non-connected automated vehicles are imperfect and there is mismatch between the model used in analytical derivation and that in simulation, the proposed adaptive driving strategy suppresses disturbances in a wide range of situations.
Keywords: car following; string stability; heterogeneous platoon; mixed traffic; vehicle-infrastructure communication; cooperative driving; automated vehicles

*Author's version. Please cite this paper as: **Wang, M. Infrastructure assisted adaptive driving to stabilise heterogeneous vehicle strings Transportation Research Part C: Emerging Technologies , 2018, Vol. 91, pp. 276 - 295**.

1 Introduction

Automated vehicles have attracted considerable attention from the public since they may completely change the way we operate our vehicles today and consequently may have great implications for the traffic operations. It is therefore important to design such systems in a scrutinized manner to ensure benefits to the traffic systems. Automated vehicles can be classified as non-connected/autonomous and connected/cooperative vehicle systems. Non-connected automated vehicles (NAVs) rely solely on on-board sensors [VanderWerf et al., 2001, Kesting et al., 2008, Xiao and Gao, 2011, Mullakkal-Babu et al., 2016], while connected automated vehicles (CAVs) exchange (e.g. output, state or control) information with each other via Vehicle-to-Vehicle (V2V) communication or with road infrastructure via Vehicle-to-Infrastructure (V2I) communication to improve situation awareness and/or to manoeuvre together under a common goal [Varaiya and Shladover, 1991, Van Arem et al., 2006, Wang et al., 2014b, Ge and Orosz, 2014, Wang et al., 2015, Milanés and Shladover, 2014].

Adaptive Cruise Control (ACC) is one of the earliest NAV systems, which is designed to enhance driving comfort [VanderWerf et al., 2001]. The most widely used ACC systems is based on linear state feedback control, where the controlled acceleration is proportional to the deviation of the gap from a desired value under the constant time gap (CTG) policy and the speed error, i.e. the relative speed with respect to the preceding vehicle [VanderWerf et al., 2001, Ploeg et al., 2014].

One of the problems with autonomous ACC is the string instability, i.e. tracking errors in one vehicle can be amplified when propagating in a platoon. The major influencing factors for vehicular string stability properties are the system properties, notably time delays of the vehicle dynamic system, and control (design) parameters, e.g. the desired gap and feedback gains. Two types of system delays can be distinguished, being sensor delay and actuator lag [Xiao and Gao, 2011, Wang et al., 2016c]. Sensor delay is caused by the process of sensing and filtering, due to the discrete sampling of on-board measurements, the radar or lidar filtering, and the bandwidth of low pass filters used for other sensors such as wheel speed sensors [Xiao and Gao, 2011, Wang et al., 2017]. The actuator lag lies in the lower level of the vehicle control system when executing the desired acceleration command from the upper level ACC controller, due to the time delay in the generation of traction/brake wheel torques in the power-train or brake actuator [Xiao and Gao, 2011].

Much work on control design and stability analysis of NAV/CAV platoons did not explicitly address both time delays [Wang et al., 2014a, Ge and Orosz, 2014, Jia and Ngoduy, 2016, Zhang and Orosz, 2016, Zhou et al., 2017, Talebpour and Mahmassani, 2016]. Omitting the combination of sensor delay and actuator lag in the control loop may result in over-optimistic evaluations of the controller performance and the corresponding impacts on traffic flow [Wang et al., 2016c]. Few studies addressed both sensor delay and actuator lag, but are restricted to the linear feedback control law with the CTG policy [Xiao and Gao, 2011]. String stability conditions of autonomous vehicle platoons employing general nonlinear gap policies with both sensor delay and actuator lag remain largely unresolved.

With V2V communication, cooperative ACC (CACC) systems that use information of platoon leader, multiple predecessor or the acceleration of the direct predecessor in addition to on-board measurements lead to enhanced string stability performance. As a result, CACC can maintain much shorter time gaps compared to ACC systems and has potential to increase roadway capacity [Van Arem et al., 2006, Shladover et al., 2012, Milanés and Shladover, 2014, Jia and Ngoduy, 2016]. The fact that CACC leads to enhanced string stability properties with information from multiple predecessors is that the additional term in the control law works as a feedforward term and compensates system delays effectively [Treiber et al., 2006]. However, CACC systems require CAVs following each other in a platoon. At low market penetrations rates, the probability of CACC vehicles forming a platoon in an ad-hoc way is very low and the potentials of the CACC system are thus confined. To circumvent the problem, a few approaches have been proposed, including variant of CACC systems that seek consensus control decisions using multiple vehicles ahead in a heterogeneous fashion [Ge and Orosz, 2014, Ngoduy, 2015, Monteil et al., 2014] or optimize platoon performance looking at not only the vehicles in front but also (human-driven) followers [Wang et al., 2014b, Wang et al., 2016b]. However, this still requires substantial penetration rates of equipped vehicles to enable the connectivity. Otherwise, the variant CACC system based on V2V communication will only generate traffic benefits at low probabilities.

Parallel to V2V based systems, another paradigm in cooperative traffic systems aims to connect traffic control with vehicle control with V2I/I2V communication, using CAVs as distributed sensors [Hegyi et al., 2013] and actuators [Wang et al., 2016a]. The combination of the aforementioned problem and the V2I/I2V based traffic control paradigm leads to the main objective of this contribution: to design an adaptive driving strategy for CAVs in mixed vehicular strings to attenuate disturbances at low market penetration rates under *vehicle-infrastructure cooperation*. We assume that a roadside system with V2I communications receives control parameters of CAVs in a string and estimates car-following parameters (imperfectly) of non-connected human-driven/automated vehicles. Given this assumption, the key is to determine the control parameters of the CAV to suppress a downstream disturbance and send them to the CAV via communication. The CAV changes its behaviour based on the adaptive parameters *commanded* by the road infrastructure. The CAV restores its default parameters once the disturbance is attenuated.

The adaptive driving strategy is based on string stability analysis of vehicle strings around equilibria. We derive sufficient conditions for string stability of a general heterogeneous platoon with mixed vehicle classes and different parameter settings. To this end, linearised vehicle system dynamics model and the acceleration control law is used in control parametrisation and Laplace transform of the speed and gap error dynamics in time domain to frequency domain enables the determination of sufficient string stability criteria of a heterogeneous vehicle string. The sufficient conditions give new insights into the relationship between the string stability properties, the system properties of time delays and controller design parameters of feedback gains and desired time gap. The sufficient conditions further allow the quantification of a stability margin, which is subsequently used to parametrise the feedback control gains and desired time gap of the CAV to suppress the amplification of gap and speed errors in a platoon.

The proposed approach is applied to examine the influence of control design parameters and system delays on the resulting string stability of ACC vehicles and to find the adaptive parameter range of adaptive driving to stabilise a vehicle string passing a disturbance that is unstable otherwise. We verify the analytical results with simulation of vehicle strings subject to exogenous disturbance, parameter estimation error and modelling uncertainties, assuming the infrastructure has *imperfect* knowledge on behaviours of non-connected vehicles in the platoon.

The remainder of the paper is organized as follows: Section 2 introduces the model for longitudinal vehicle dynamics. Section 3 presents the string stability conditions for homogeneous vehicle strings with two delays and a generalised gap policy, followed by the extension to string stability conditions for heterogeneous strings in Section 4. Section 5 focuses on the string stability margin and the conditions for the adaptive driving strategy to stabilise a mixed string. We summarise the study in Section 6.

2 Vehicle longitudinal dynamics model

Let x_i denote the longitudinal position of vehicle i in a platoon, which increases in the forward driving direction, then its longitudinal dynamics can be expressed as (for simplicity we drop the time argument):

$$m\ddot{x}_i = \underbrace{F_i}_{\text{tractive force}} - \underbrace{R_{a,i}}_{\text{aerodynamic drag}} - \underbrace{R_{g,i}}_{\text{grade resistance}} - \underbrace{R_{d,i}}_{\text{mechanical drag}} \tag{1}$$

Equation (1) represents Newton's second law applied to vehicle i as a point mass. m_i denotes the vehicle mass and F_i denotes engine force applied to the vehicle.

The basic equation (1) is nonlinear due to aerodynamic drag $R_{a,i}$. Employing the exact linearisation technique detailed in Appendix A allows us to model the longitudinal vehicle dynamics in a linear form as [Sheikholeslam and Desoer, 1993, Xiao and Gao, 2011]:

$$\frac{\mathrm{d}}{\mathrm{d}t}\begin{pmatrix} x_i \\ \dot{x}_i \\ \ddot{x}_i \end{pmatrix} = \begin{pmatrix} \dot{x}_i \\ \ddot{x}_i \\ \frac{u_i - \ddot{x}_i}{\tau_i} \end{pmatrix} \tag{2}$$

Here u_i denotes the control input, which can be interpreted as the *desired acceleration* of vehicle i. The time constant τ_i represents the engine actuator lag, implies that *the commanded acceleration u_i cannot be realized instantaneously* but only after a retarded time τ_i. The linearised model enables us to analyse the properties of the feedback ACC/CACC control law without consideration of the lower-level complexity.

Remark 2.1 *The linearised model in frequency domain is:*

$$V(z) = \frac{1}{\tau_i z + 1} \tag{3}$$

The actuator lag functions as a low pass filter.

Remark 2.2 *Note that, quite some studies ignore the actuator delay in modelling and control design. As we will show later, this may lead to instability at high frequencies as an artifact of ignoring the actuator lag.*

For autonomous car-following control of vehicle i, it is convenient to define the system state such that it couples the dynamics of the predecessor $i-1$. Hence, we define the system state (vector) $\mathbf{X}$ as: $\mathbf{X} = (s_i, v_{i-1}, v_i, a_i)$, where $s_i = x_{i-1} - x_i - l_i$ denotes the gap or spacing with respect to the preceding vehicle $i-1$, l_i denotes the vehicle length. For state-feedback control laws, the control input u_i can be expressed as an explicit functional of the state vector: $u = f(\mathbf{X})$. The state variables can be measured/estimated from

on-board sensors of vehicle i but are subject to a time delay ξ_i. Hence when including state delay, the system dynamics can be written as:

$$\frac{\mathrm{d}}{\mathrm{d}t}\mathbf{X}(t) = \frac{\mathrm{d}}{\mathrm{d}t}\begin{pmatrix} s_i(t) \\ v_{i-1} \\ v_i(t) \\ a_i(t) \end{pmatrix} = \begin{pmatrix} \Delta v_i(t) \\ a_{i-1}(t) \\ a_i(t) \\ \frac{u_i(t)-a_i(t)}{\tau_i} \end{pmatrix} = \begin{pmatrix} \Delta v_i(t) \\ a_{i-1}(t) \\ a_i(t) \\ \frac{f(\mathbf{X}_i(t-\xi_i))-a_i(t)}{\tau_i} \end{pmatrix} \tag{4}$$

where $\Delta v_i := v_{i-1} - v_i$ denotes the relative speed with respect to the preceding vehicle.

3 String stability of homogeneous platoon with feedback delay and mechanical lag

In this section, we examine the string stability criteria for homogeneous platoons with sensor delay and actuator lag.

3.1 General control law and equilibria

Due to low signal-to-noise ratio of the vehicle acceleration measurements from on-board sensors, it is not desirable to include acceleration variable a_i in the feedback control law for NAVs. Hence a general formulation of a nonlinear control law in state feedback form can be written as:

$$u_i(t) = f(\mathbf{X}_i(t-\xi_i)) = f(s_i(t-\xi_i), v_i(t-\xi_i), v_{i-1}(t-\xi_i)) \tag{5}$$

Inserting the feedback law (5) into the system dynamics equation (4) we get the compact description of the closed-loop system dynamics as:

$$\dot{a}_i(t) = \frac{f(s(t-\xi_i), v_i(t-\xi_i), v_{i-1}(t-\xi_i)) - a_i(t)}{\tau_i} \tag{6}$$

For car-following control, a desired gap $s_{d,i}$ is usually defined under some desired gap/spacing policy. The general (nonlinear) gap policy is described as a non-decreasing function of vehicle speed:

$$s_{d,i} = \mathfrak{g}_i(v_i) \tag{7}$$

The main control objective for the car-following controller for vehicle i is to track the predecessor with the desired gap and with zero relative speed. Hence, at equilibria, all vehicles in a string travel at the same speed v_e and at their desired gaps $s_{e,i} = \mathfrak{g}_i(v_e)$, and the desired and actual accelerations are thus equal to zero, i.e. $u_{e,i} = a_{e,i} = 0$.

3.2 Definition of string stability of homogeneous platoon

Before we detail the stability analysis approach, we first define the string stability we use throughout this paper.

Definition 3.1 *Let y denote the signal of interest, e.g. disturbance in speed or gap, and let Γ denote the frequency response function between the scalar output y_{i-1} of the preceding vehicle $i-1$ and the scalar output y_i of the follower i, i.e. $\Gamma_i(z) \equiv \frac{Y_i(z)}{Y_{i-1}(z)}$. A string of length m is said to be string stable if the condition*

$$\sup|\Gamma_i(z)| = \sup_{\omega>0}|\Gamma_i(j\omega)| \leq 1 \ , \ 2 \leq i \leq m \tag{8}$$

holds for all frequencies of $\omega > 0$.

z denotes the complex variable of frequency in this paper. Definition 3.1 states that the disturbance of the signal of interest will not be amplified when propagating along the considered string.

It is worth mentioning that there are different definitions of string stability in literature [Naus et al., 2010, Ploeg et al., 2014]. While acknowledging that our definition of string stability is based on the system output or performance, the string stability/instability concept we use in this paper has been proved to be quite relevant for macroscopic traffic flow phenomena such as stop-and-go waves [Wilson, 2008, Treiber and Kesting, 2011]. Moreover, both speed and gap disturbances have been used as signals in determining string stability conditions in literature. However, we remark that the string stability conditions derived from speed disturbance and gap disturbance are only the same in homogeneous platoons, not in heterogeneous platoons as we will show in Section 4. Gap disturbance propagation function is derived from the speed disturbance propagation function but is more generic and complex than the latter. Therefore, we use gap disturbance as the signal y to determine stability condition.

3.3 Speed error transfer function

To get the speed error transfer function, we first approximate the general control law (5) around equilibria:

$$f(s_i(t-\xi_i), v_i(t-\xi_i), v_{i-1}(t-\xi_i)) \approx f_{s_i}\tilde{s}(t-\xi_i) + f_{v_i}\tilde{v}_i(t-\xi_i) + f_{v_{i-1}}\tilde{v}_{i-1}(t-\xi_i) \tag{9}$$

where $\tilde{s}_i = s_i - s_e$, $\tilde{v}_i = v_i - v_e$ and $\tilde{v}_{i-1} = v_{i-1} - v_e$ denote the small perturbations in equilibrium gap and equilibrium speeds respectively and $f_{s_i} = \frac{\partial f}{\partial s_i}|_{v_e}$, $f_{v_i} = \frac{\partial f}{\partial v_i}|_{v_e}$, $f_{v_{i-1}} = \frac{\partial f}{\partial v_{i-1}}|_{v_e}$ are evaluated at equilibria. Inserting (9) into (6) and differentiating both sides of (6) arrives at:

$$\ddot{a}(t) = \frac{f_{s_i}(\tilde{v}_{i-1}(t-\xi_i) - \tilde{v}_i(t-\xi_i)) + f_{v_i}a_i(t-\xi_i) + f_{v_{i-1}}a_{i-1}(t-\xi_i) - \dot{a}_i(t)}{\tau_i} \tag{10}$$

Assuming zero initial conditions for speeds and accelerations, applying Laplace transform and rearranging the resultant equation gives the speed error transfer function in frequency domain as:

$$G_i(z) = \frac{V_i(z)}{V_{i-1}(z)} = \frac{(f_{v_{i-1}}z + f_{s_i})e^{-\xi_i z}}{\tau_i z^3 + z^2 - f_{v_i}e^{-\xi_i z}z + f_{s_i}e^{-\xi_i z}} \tag{11}$$

Equation (11) represents the speed disturbance propagation from the immediate predecessor to the follower.

3.4 Gap error transfer function

Given a general nonlinear gap policy of Eq. (7), the gap error is defined as:

$$e_{s,i} = s_i - \mathfrak{g}_i(v_i) \tag{12}$$

Differentiating the above equation gives

$$\dot{e}_{s,i} = v_{i-1} - v_i - z\dot{\mathfrak{g}}_i(v_i) = v_{i-1} - v_i - z\frac{\mathrm{d}\mathfrak{g}_i}{\mathrm{d}v_i}\frac{\mathrm{d}v_i}{\mathrm{d}t} = v_{i-1} - v_i - z\mathfrak{g}_i'(v_i)a_i \tag{13}$$

Note that the sensitivity function $\mathfrak{g}_i'(v_i) = \frac{d\mathfrak{g}_i}{dv_i}$ [Treiber and Kesting, 2013] has physical meanings, i.e. it represents the *desired time gap* that the controlled vehicle aims to maintain at equilibrium conditions. It is derived by equilibrium gap-speed relation by taking $e_{s,i} = 0$ and taking derivative with respect to v_i.

Performing Laplace transform to Eq. (13) and assuming zero initial conditions, we get:

$$zE_{s,i}(z) = V_{i-1}(z) - V_i(z) - zV_i(z)\mathfrak{g}_i'(v_i) \tag{14}$$

Using the relation of $G_i(z) = \frac{V_i(z)}{V_{i-1}(z)}$ and $G_{i-1}(z) = \frac{V_{i-1}(z)}{V_{i-2}(z)}$, we arrive at the following gap error transfer function:

$$H_i(z) = \frac{E_{s,i}}{E_{s,i-1}} = G_i(z)\mathcal{G}_i(z) \tag{15a}$$

$$\mathcal{G}_i(z) = \frac{1/G_i(z) - 1 - z\mathfrak{g}_i'(v_i)}{1/G_{i-1}(z) - 1 - z\mathfrak{g}_{i-1}'(v_{i-1})} \tag{15b}$$

Equation (15) represents the gap disturbance propagation from the immediate predecessor to the follower and has the speed disturbance propagation function as one of its components.

3.5 String stability criteria

With the disturbance propagation functions derived so far, we can specify Definition 3.1 as: *string stability of a homogeneous vehicle platoon is guaranteed if:*

$$|H_i(j\omega)| < 1 \text{ for } \forall\omega > 0 \tag{16}$$

With Eq. (15) and $z = j\omega$ where $\omega \in \mathbb{R}^+$ represents the frequency, it follows naturally that:

Condition 3.2 *One sufficient condition for string stability of a general vehicle platoon is:*

$$|G_i(j\omega)| < 1 \text{ and } |\mathcal{G}_i(j\omega)| < 1 \text{ for } \forall\omega > 0 \tag{17}$$

Remark 3.3 *For homogeneous vehicle strings, where $G_i(z) = G_{i-1}(z)$ and $\mathfrak{g}_i'(v_i) = \mathfrak{g}_{i-1}'(v_{i-1})$, we have:*

$$H_i(z) = G_i(z) = \frac{(f_{v_{i-1}}z + f_{s_i})e^{-\xi_i z}}{\tau_i z^3 + z^2 - f_{v_i}e^{-\xi_i z}z + f_{s_i}e^{-\xi_i z}} \tag{18}$$

Remark 3.3 states that for homogeneous vehicle platoons, the gap error propagation is equivalent to the speed error propagation in frequency domain.

For notation simplicity, we drop the index i and use $f_{v_p} = f_{v_{i-1}}$ to represent the derivative of the predecessor in the following theorem:

Theorem 3.4 *For any given frequency $\omega > 0$, if $\mathfrak{g}_i'(v_i) > \tau_i$, the upper bound of the magnitude of the gap error transfer function for a homogeneous string is:*

$$\sup|H(j\omega)| = \sup|G(j\omega)| = \frac{f_{v_p}^2\omega^2 + f_s^2}{\tau^2\omega^6 + (1 + 2f_v\tau + 2f_s\tau\xi + 2f_v\xi)\omega^4 + (-2f_s + f_v^2)\omega^2 + f_s^2} \tag{19}$$

Proof: Appendix B

From Theorem 3.4, we derive the following two corollaries:

Corollary 3.4.1 *Sufficient string stability condition 1: The first sufficient condition for string stability of homogeneous strings with two delays derived from Theorem 3.4 is:*

$$A_2 = -2f_s + f_v^2 - f_{v_p}^2 > 0 \tag{20a}$$

$$A_4 = 1 + 2f_v\tau + 2f_s\tau\xi + 2f_v\xi > 0 \tag{20b}$$

Proof: Proof of Corollary 3.4.1 is straight forward. Notice that $A_6 = \tau^2 > 0$, string stability requires $\sup|H(jw)| < 1$, which is unconditionally satisfied if $A_4 = 1 + 2f_v\tau + 2f_s\tau\xi + 2f_v\xi > 0$ and $-2f_s + f_v^2 > f_{v_p}^2$ (or equivalently $A_2 = -2f_s + f_v^2 - f_{v_p}^2 > 0$)

Notice that Corollary 3.4.1 can be seen as a generalization of previous work on homogeneous string stability analysis for ACC systems [Xiao and Gao, 2011, Zhou and Peng, 2005] since it covers more general nonlinear gap policies.

It can also be regarded as a generalization of previous work on string stability of homogeneous human car-following models without explicit time delays, since when $\tau = \xi = 0$, Condition (20b) is always respected and (20a) is exactly the string stability criterion for homogeneous car-following models without time delays [Wilson, 2008, Treiber and Kesting, 2011].

Conditions (20a,20b) give the relations between model/design parameters (embedded in the partial derivatives of the acceleration model/controller) and the two delays, which can be used for control parametrisation, c.f. Section 3.6. The very existence of the second condition (20b) implies that the string stability condition for systems with delay is stricter than those without delay.

Corollary 3.4.2 *Sufficient string stability condition 2: a second sufficient condition for string stability derived from Theorem 3.4 is:*

$$A_4 < 0 \text{ and } A_2 > \frac{A_4^2}{4A_6} \tag{21}$$

Proof: If $A_4 < 0$, $|H(z)| < 1$ can still be respected if

$$\tau^2\omega^6 + (1 + 2f_v\tau + 2f_s\tau\xi + 2f_v\xi)\omega^4 + (-2f_s + f_v^2)\omega^2 > f_{v_p}^2\omega^2 \tag{22}$$

Equivalently, we can solve the following polynomial inequality:

$$\min_{\omega>0} Y(\omega) = A_6\omega^4 + A_4\omega^2 + A_2 > 0 \ , \forall\omega > 0 \tag{23}$$

with $A_6 = \tau^2 > 0$. One can find the roots of the polynomial with $\frac{\partial Y(\omega)}{\partial\omega} = 0$ and $\omega > 0$, which gives

$$\omega^* = \pm\sqrt{\frac{-A_4}{2A_6}} \text{ or } \omega^* = 0 \tag{24}$$

Removing the negative and zero roots of ω and inserting ω^* to Y we arrive at:

$$\min_{\omega>0} Y(\omega) = A_6\left(\sqrt{\frac{-A_4}{2A_6}}\right)^4 + A_4\left(\sqrt{\frac{-A_4}{2A_6}}\right)^2 + A_2 > 0 \tag{25}$$

which will be respected if $A_2 > \frac{A_4^2}{4A_6}$. Note that Corollary 3.4.2 has not been discovered in previous work [Xiao and Gao, 2011, Zhou and Peng, 2005]

In the remainder of this section, we will demonstrate the applicability of the analytical conditions for parameters design of ACC systems.

3.6 Worked example: Linear ACC controller with CTG policy

Let us exemplify the applicability of the analytical approach in parametrising the widely used linear ACC controller for NAVs with the CTG policy [VanderWerf et al., 2001, Shladover et al., 2015] as:

$$u_i = k_v e_{v,i} + k_s e_{s,i} = k_v(v_{i-1} - v_i) + k_s(s_i - v_i * t_d - s_0) \tag{26}$$

with sensor delay ξ_i and actuator lag τ_i. k_v and k_s are feedback gains on speed error and gap error respectively and t_d is the constant desired time gap. s_0 denotes the gap at standstill conditions.

Note that Eq. (26) is not a complete ACC since it does not cover approaching mode and collision avoidance mode [Xiao et al., 2017]. When designing state feedback controllers that incorporate full operating modes for longitudinal control, the feedback gains on gap and speeds should not be set at constant, but rather dependent on state [Wang et al., 2014a, Kesting et al., 2008].

The derivatives of the control law are given as:

$$f_s = k_s,\ f_{v_p} = k_v,\ f_v = -k_v - k_s * t_d \tag{27}$$

The gap/speed error transfer function 11 is specified as

$$H(z) = G(z) = \frac{(k_v z + k_s)e^{-\xi_i z}}{\tau_i z^3 + z^2 + (k_v + t_d k_s)z e^{-\xi_i z} + k_s e^{-\xi_i z}} \tag{28}$$

with $A_2 = -2f_s + f_v^2 - f_{vp}^2 = k_s^2 t_d^2 + 2k_s k_v t_d - 2k_s$, $A_4 = (1 + 2f_v\tau + 2f_s\tau\xi + 2f_v\xi) = 1 - 2(k_v + k_s t_d)(\tau + \xi) + 2k_s\tau\xi$, $A_6 = \tau^2$.

We can plot the stability conditions in a two-dimensional plane of control and system parameters in Figures 1-3, which gives four regions:

- *Type I stability*, stable due to satisfying the first string stability condition of Corollary 3.4.1;
- *Type II stability*, stable due to satisfying the second string stability condition of Corollary 3.4.2;
- *Type I instability*, unstable due to violating $A_2 > 0$;
- *Type II instability*, unstable due to violating $A_2 > \frac{A_4^2}{4A_6}$ while $A_4 < 0$.

Note that A_2 is proportional to the (negative) second coefficient of a Taylor expansion of $|G(\omega)|$ around $\omega = 0$. This implies that Type I instability ($A_2 <= 0 \& A_4 > 0$) is a long-wavelength instability since it firstly arises for $\omega \to 0$ when crossing the instability region by changing parameters. In contrast, if $0 < A_2 < A_4^2/4/A_6$ and $A4 < 0$, the first Type II instability appears at a finite $\omega > 0$, which is short-wavelength instability. Since Type II string stability is less stricter than Type I string stability, when parametrising controller from string stability to string instability, Type I string stability vanishes first.

In the sequel, we present some interesting insights from the stability diagrams 1-3.

3.6.1 Influence of control parameters: feedback gains and desired time gap

Insights into the influence of control parameters on the string stability of a homogeneous platoon can be gained via examining the stability diagram of Figure 1 with $\xi = 0.2$ s, $\tau = 0.2$ s.

- Influence of feedback gains is *not monotonic*. When k_s is small, increasing k_s has the stabilising effect in a certain range of k_v. However, when k_s is large, increasing it may destabilise the string. Similar trend is observed for the feedback gain of speed error k_v.
- At small time gaps, e.g. $t_d = 1.0$ s, the feedback gain on speed error needs to be set high while the feedback gain on gap error needs to be set low to guarantee Type I string stability.
- When t_d is below some threshold, e.g. $t_d < 1.6$ s, increasing t_d enlarges Type I and II stability regions. However, when t_d increases further than 1.8 s, the stability regions does not increase significantly, but their positions change in the plan. The two lines (one separating Type I instability and Type I stability and the other separating Type I and Type 2 stability) becomes steeper and they shifts towards the origin with the increase of desired time gap.
- For all two instability regions, high frequency disturbances will be damped out thanks to $A_6 = \tau^2 > 0$.

Remarkably, when ignoring delays, the insights into the influence of the feedback gains are no long consistent with those with two delays. When both delays are ignored, *monotonic influence of control design parameters* emerge as shown in Figure 2:

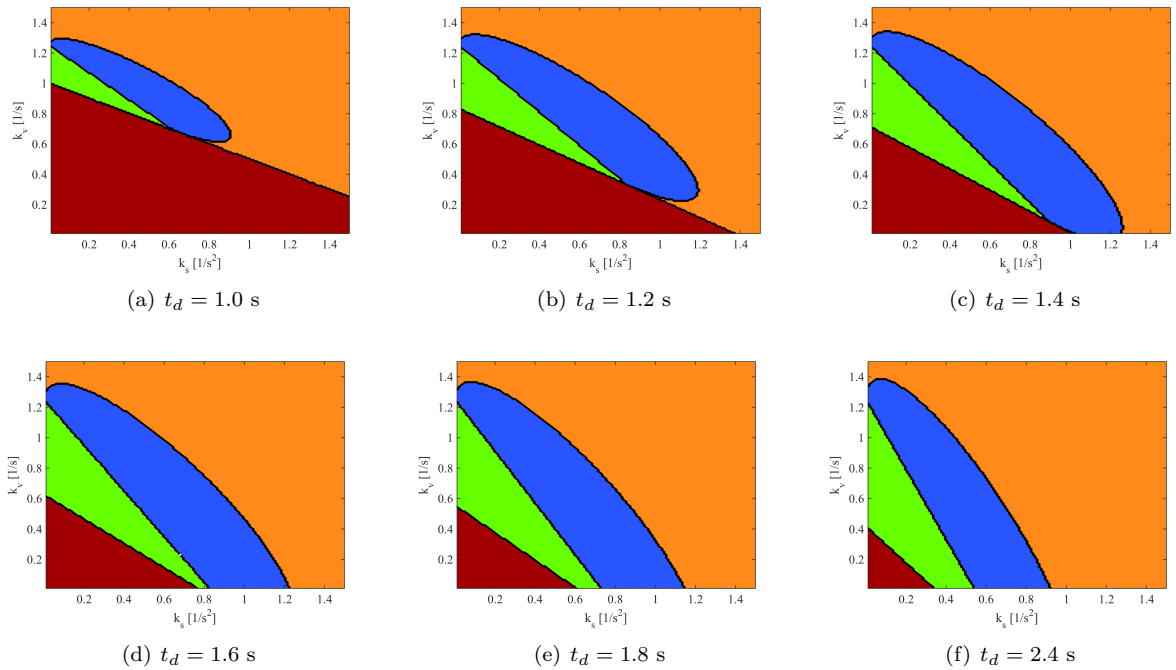

(a) $t_d = 1.0$ s (b) $t_d = 1.2$ s (c) $t_d = 1.4$ s

(d) $t_d = 1.6$ s (e) $t_d = 1.8$ s (f) $t_d = 2.4$ s

Figure 1: Stability diagram in $k_s - k_v$ plane with two delays $\xi = 0.2$ s and $\tau = 0.2$ s. Green region depicts Type I stability; blue region depicts Type II stability; red region depicts Type I instability; orange region depicts Type II instability.

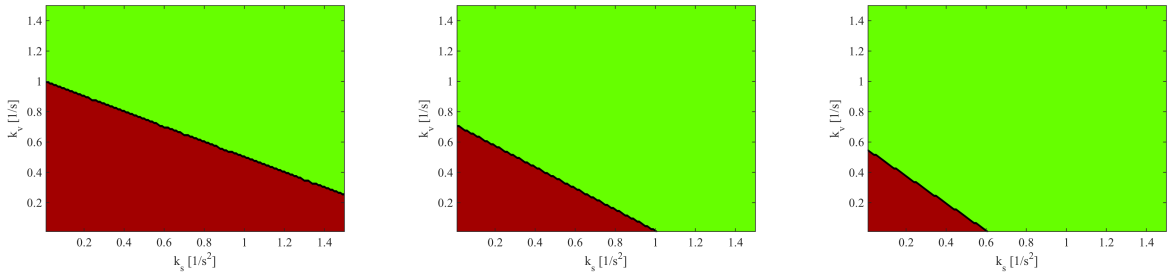

(a) $t_d = 1.0$ s (b) $t_d = 1.4$ s (c) $t_d = 1.8$ s

Figure 2: Stability diagram in $k_s - k_v$ plane with with zero delays $\xi = 0$ s and $\tau = 0$ s. Green region depicts Type I stability; red region depicts Type I instability.

- $A_4 > 0$ is unconditionally respected and only $A_2 > 0$ is needed to guarantee string stability;
- Type II stability and instability regions cannot be identified;
- Increasing t_d will always increase the string stability region;
- Increasing k_s and k_v will always stabilise the string, which will invalidated by simulation in the simulation experiments.
- High frequency disturbance will be damped out due to $A_4 = 1$ and $A_6 = 0$.

We remark here that designing ACC systems without considering system (sensor and actuator) delays may lead to over-estimate of the benefits of ACC systems on traffic flow stability due to the monotonic influence of design parameters on string stability.

3.6.2 Influence of system properties: sensor delay and actuator lag

Without any delay, only $A_2 > 0$ is needed to guarantee string stability and the larger A_2, the smaller the magnitude of the transfer function (19). In this case, increasing k_v and k_s will certainly increase string stability, as shown in Figure 2. However, this is not the case when considering delays. The stabilising effect of increasing feedback gains of k_v and k_s only works in certain regions, but not in all regions, cf. Figure 1.

This implies that delays may have negative effects on string stability. Below we analytically impart the intuition of the influence of two delays on string stability. We show in Eq. (71) in Appendix that $f_v + f_s\tau < 0$. The same procedure can be used to derive the relation between f_s and ξ as:

$$f_v + f_s\xi < 0 \tag{29}$$

Using these two relations, Condition 20b can be rewritten as:

$$A_4 = 1 + 2(f_v + f_s\tau)\xi + 2f_v\tau = 1 + 2(f_v + f_s\xi)\tau + 2f_v\xi > 0 \tag{30}$$

Note that $f_v < 0$, hence increasing the value of τ and ξ tends to violate Condition 20b, thus deteriorates string stability. The relative change is the same for τ and ξ in Eq. (30) since it is symmetric in both parameters.

Nevertheless, increasing τ also increase the coefficient of the higher order term A_6 in (19), which has a stabilising effect. Thus the destabilisation effect is less serious for increasing τ than the same magnitude of increase in ξ. When the frequency of the disturbance is high enough, e.g. higher than the system and control parameters (which are often less than 2), A_6 even circumvents the destabilising effect of τ and becomes the major determinant of the resulting string stability.

Figure 3 depicts the supreme of the magnitude of the gap error transfer function (19) at different frequencies in the two dimension-plane of τ and ξ. As we can see from the figure:

- At low disturbance frequencies (e.g., $\omega <= 0.1$ rad/s), increasing delay or actuator lag tends to increase the magnitude of the gap error transfer function and consequently destabilises vehicle strings.
- At high frequencies (e.g., $\omega > 1$), the higher order term $\tau^2\omega^6$ will dominate the magnitude of the transfer function and increasing actuator lag tends to stabilise the string while increasing sensor delay always tends to destabilise vehicle strings.
- At mediate frequencies, e.g. $w = 0.8$ rad/s, increasing sensor delay will destabilise the string. Increasing actuator lag will first deteriorate string stability performance, but after a certain level, it will tend to stabilise the string. This clearly shows the trade off between the destabilising effect of the 4th order term and stabilising effect of the 6th order term with the increase of τ.

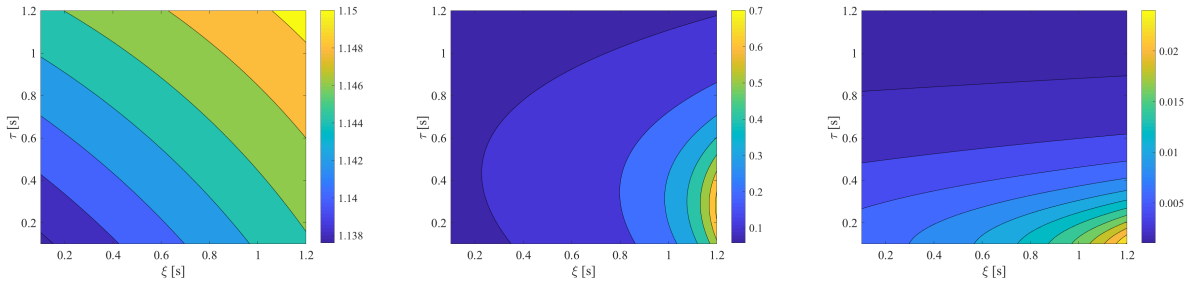

(a) Magnitude at $\omega = 0.1$ rad/s (b) Magnitude at $\omega = 0.8$ rad/s (c) Magnitude at $\omega = 2$ rad/s

Figure 3: Magnitude contour plot in $\xi - \tau$ plane at different frequencies with $k_s = 0.1$, $k_v = 0.15$, $t_d = 1.5$

3.7 Verification by simulation

The stability diagrams shown so far give an intuitive means to design control parameters for string stability. To verify the analytical results, we simulate a platoon of 6 vehicles of which 5 ACC followers employing the linear ACC control law follows an exogenous leader. We impose step deceleration disturbance followed by acceleration disturbance of the leader (see leader acceleration profile in Figure 4). We test different k_s and k_v combinations at the desired time gap of $t_d = 1.2$ s to generate stable string (Figure 4(a)), unstable string with Type I instability (Figure 4(d)) and unstable string with Type II instability (Figure 4(g)) as predicted by Corollary 3.4.1 and 3.4.2. The vehicle accelerations and the gap errors in the scaled the position of the vehicles in the platoon for the three platoons are shown in Figure 4(b)4(c), 4(e)4(f), 4(h)4(i) respectively.

The acceleration and gap error plots verify the analytical predictions, in particular the long-wavelength feature of Type I instability and short-wavelength feature of Type II instability. Note that Type II instability is associated with many local oscillations. This is certainly not desired from controller design perspective.

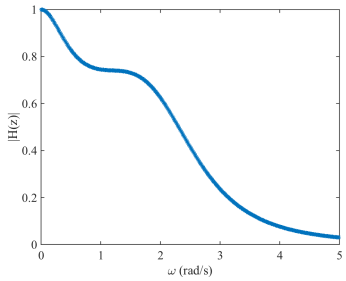

(a) Magnitude of gap error transfer function under string stability with $k_s = 0.6$, $k_v = 0.8$, and $t_d = 1.2$

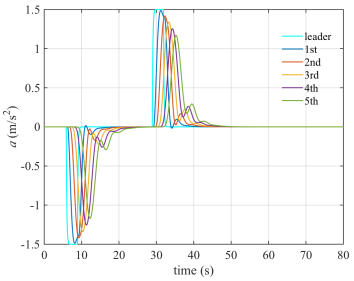

(b) Acceleration profiles under string stability

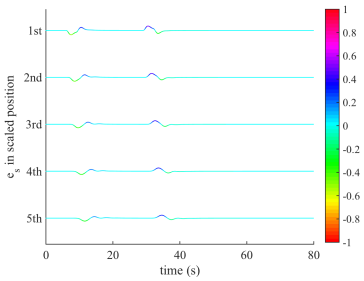

(c) Gap error propagatation under string stability

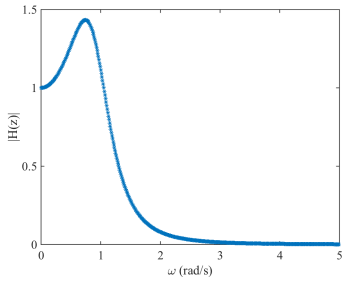

(d) Magnitude of gap error transfer function under Type I instability with $k_s = 0.6$, $k_v = 0.2$, and $t_d = 1.2$

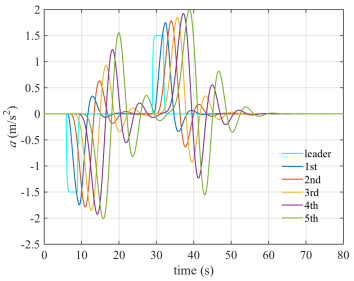

(e) Acceleration profiles under Type I instability

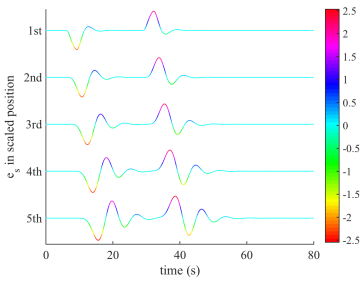

(f) Gap error propagatation under Type I instability

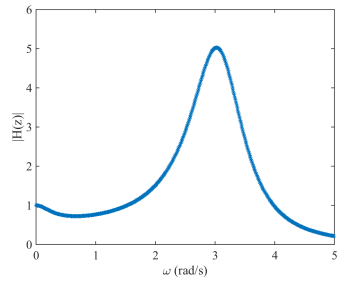

(g) Magnitude of gap error transfer function under Type II instability with $k_s = 0.6$, $k_v = 1.5$, and $t_d = 1.2$

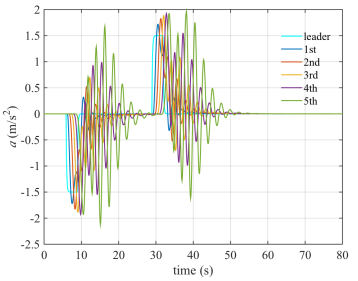

(h) Gap error under Type II instability

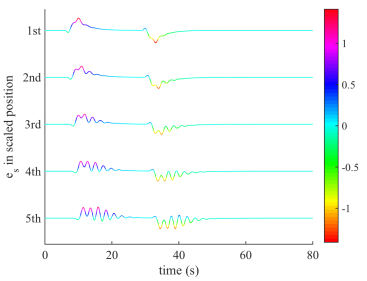

(i) Gap error propagatation under Type II instability

Figure 4: Magnitude as a function of frequency under different parameter settings

4 String stability condition of heterogeneous platoon

The previous section lays the foundation for string stability analysis by deriving conditions for homogeneous strings. This section goes a step further to string stability condition of heterogeneous platoon with different control parameters and system properties.

4.1 Strict and weak string stability: definition

For vehicle string with heterogeneous system and control parameters, string stability can be examined by the transfer function of the gap error from the first follower to the last follower. For a heterogeneous platoon of length k, we can distinguish between string and weak string stability concepts. For strict string stability, we require the magnitude of the gap error transfer function in each predecessor-follower pair in the platoon less than unity:

$$|H_i(z)| = \left| \frac{E_{s,i}(z)}{E_{s,i-1}(z)} \right| < 1, \forall i \leq k \tag{31}$$

Derivation of strict string stability condition is straightforward in the sense that one can apply Corollary 3.4.1 and 3.4.2 to each predecessor-follower pair. Condition (31) is rather strict whereas in a heterogeneous string setting, disturbances amplified by a string-unstable predecessor-follower pair can be damped out by an upstream string-stable predecessor-follower pair. Hence, a weak string stability concept is defined as:

$$|\bar{H}_{1-k}(z)| = \left| \frac{E_{s,k}(z)}{E_{s,1}(z)} \right| < 1 \tag{32}$$

The weak string stability is also referred to as head-to-tail string stability [Ge and Orosz, 2014]. In the sequel, We employ this definition to derive the analytical string stability criterion for heterogeneous platoons with length k.

The finite length platoon setting allows us to define the head-to-tail string stability, which has practical implications in damping disturbance in mixed traffic. While not being able to directly control the behaviour of human-driven vehicles, adapting the behaviour of a small number of controlled vehicles in a mixed platoon may guarantee that the amplitude at the tail of a finite platoon is smaller than that of the head. Repeating this throughout the whole traffic with randomly distributed controlled vehicles can damp out the disturbance in traffic.

4.2 Conditions for strict and head-to-tail string stability

Given a general nonlinear gap policy of Eq. 7, the gap error function of the 1st and the kth vehicle is:

$$\begin{aligned} e_{s,1} &= x_0 - x_1 - l_1 - \mathfrak{g}_1(v_1) && \text{(33a)} \\ e_{s,k} &= x_{k-1} - x_k - l_k - \mathfrak{g}_k(v_k) && \text{(33b)} \end{aligned}$$

where l_k is the length of vehicle k. Here we use $\mathfrak{g}_k$ to differentiate the gap policies of vehicles in the heterogeneous string, whereas in literature, most of them refer to a homogeneous gap policy.

Differentiating the above equation arrives at:

$$\begin{aligned} \dot{e}_{s,1} &= v_0 - v_1 - \mathfrak{g}_1'(v_1)a_1 \\ \dot{e}_{s,k} &= v_{k-1} - v_k - \mathfrak{g}_k'(v_k)a_k \end{aligned} \tag{34}$$

Performing Laplace transform to the above equation and using the relation of $G_i(z) = \frac{V_i(z)}{V_{i-1}(z)}$ we can get:

$$H_i(z) = \frac{E_{s,i}}{E_{s,i-1}} = G_i(z) \frac{1/G_i(z) - 1 - z\mathfrak{g}_i'(v_i)}{1/G_{i-1}(z) - 1 - z\mathfrak{g}_{i-1}'(v_{i-1})} \tag{35}$$

The head-to-tail gap error propagation function $\bar{H}_{1-k}(z)$ is:

$$\begin{aligned} \bar{H}_{1-k}(z) &= \frac{E_{s,k}}{E_{s,1}} = \frac{E_{s,k}}{E_{s,k-1}} \cdot \frac{E_{s,k-1}}{E_{s,k-2}} \cdot ... \cdot \frac{E_{s,2}}{E_{s,1}} = \prod_{j=1}^{k} H_j(z) \\ &= \frac{1/G_k(z) - 1 - z\mathfrak{g}_k'(v_k)}{1/G_0(z) - 1 - z\mathfrak{g}_0'(v_0)} \prod_{j=1}^{k} G_j(z) \end{aligned} \tag{36}$$

where the speed error transfer function $G_i(z)$ is defined in Eq. (11).

Strict string stability is guaranteed if:

$$|H_i(j\omega)| \leq \left| \frac{1/G_i(z) - 1 - z\mathfrak{g}_i'(v_i)}{1/G_{i-1}(z) - 1 - z\mathfrak{g}_{i-1}'(v_{i-1})} \right| |G_i(z)| < 1, \forall \omega > 0 \text{ and } \forall i \in [1, k] \tag{37}$$

Head-to-tail string stability is guaranteed if:

$$|\bar{H}_{1-k}(j\omega)| \leq \left| \frac{1/G_k(j\omega) - 1 - j\omega \mathfrak{g}'_k(v_k)}{1/G_0(\omega) - 1 - j\omega \mathfrak{g}'_0(v_0)} \right| \prod_{j=1}^{k} |G_j(j\omega)| < 1, \forall \omega > 0 \tag{38}$$

Since we have derived the upper bound of the speed error transfer function $G(z)$ in (19), this gives the following *sufficient condition for strict string stability* as:

Condition 4.1 *Strict string stability for heterogeneous vehicle string is guaranteed if:*

$$\left| \frac{1/G_i(j\omega) - 1 - z\mathfrak{g}'_i(v_i)}{1/G_{i-1}(j\omega) - 1 - z\mathfrak{g}'_{i-1}(v_{i-1})} \right| < 1 \tag{39a}$$

$$\frac{f_{v_{i-1}}^2 \omega^2 + f_{s_i}^2}{\tau_i^2 \omega^6 + (1 + 2f_{v_i}\tau_i + 2f_s\tau_i\xi_i + 2f_{v_i}\xi_i)\omega^4 + (-2f_{s_i} + f_{v_i}^2)\omega^2 + f_{s_i}^2} < 1 \tag{39b}$$

for $1 \leq i \leq k$ *and* $\mathfrak{g}'_i(v_i) > \tau_i$.

Similarly, we can get the following *sufficient condition for head-to-tail string stability* as:

Condition 4.2 *Head-to-tail string stability is guaranteed if:*

$$\left| \frac{1/G_k(j\omega) - 1 - z\mathfrak{g}'_k(v_k)}{1/G_0(j\omega) - 1 - z\mathfrak{g}'_0(v_0)} \right| < 1 \tag{40a}$$

$$\frac{f_{v_{i-1}}^2 \omega^2 + f_{s_i}^2}{\tau_i^2 \omega^6 + (1 + 2f_{v_i}\tau_i + 2f_s\tau_i\xi_i + 2f_{v_i}\xi_i)\omega^4 + (-2f_{s_i} + f_{v_i}^2)\omega^2 + f_{s_i}^2} < 1 \tag{40b}$$

for $1 \leq i \leq k$ *and* $\mathfrak{g}'_i(v_i) > \tau_i$.

If the model parameters are known, Eqs. (39a,40a) can be numerically calculated using Padé approximation.

4.3 Verification by simulation

To verify the sufficient conditions for strict and head-to-tail string stability, we simulate three heterogeneous platoons of four vehicles with three ACC followers employing different control parameters following an exogenous leader under the same periodic speed disturbance (see leader speed profiles in Figure 5(b),6(b),7(b)). We choose the control parameters such that the three platoons exhibit strict string stability (see Figure 5), head-to-tail string stability (see Figure 6) and string instability (see Figure 7) according to analytical prediction respectively.

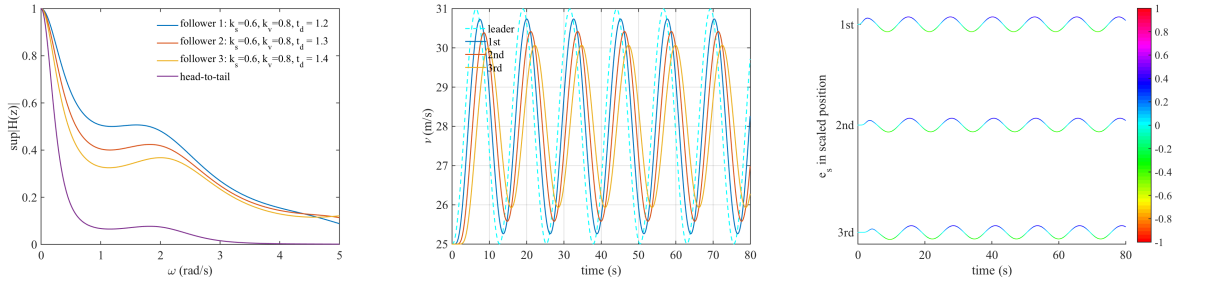

(a) analytical prediction in frequency domain

(b) speed in time domain

(c) gap error propagation with relative position of vehicles

Figure 5: Example 1: strict string stability of heterogeneous platoon under periodic leader disturbance

Figure 5(a) shows the strict string stability, where the magnitudes of the gap error transfer functions for all followers are less than unity. The simulation confirms the analytical prediction, as we can see clearly from Figure 5(b)5(c) that the disturbance in gap error and speed is attenuated monotonically when propagating along the platoon. Figure 6(a) shows the head-to-tail string stable case, where follower 2 is a string destabiliser but head-to-tail magnitude is less than unity. Speed and gap error dynamics in time domain in Figure 6(b)6(c) verify the analytical prediction. Figure 7(a) shows the string unstable case and is verified by simulations in Figure 7(b)7(c).

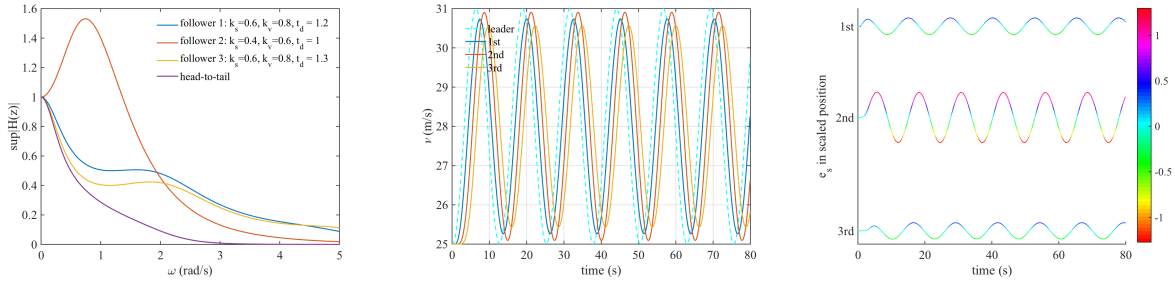

(a) analytical prediction (b) speed in time domain (c) gap error propagation with relative position of vehicles

Figure 6: Example 2: weak/head-to-tail string stability of heterogeneous platoon under periodic leader disturbance

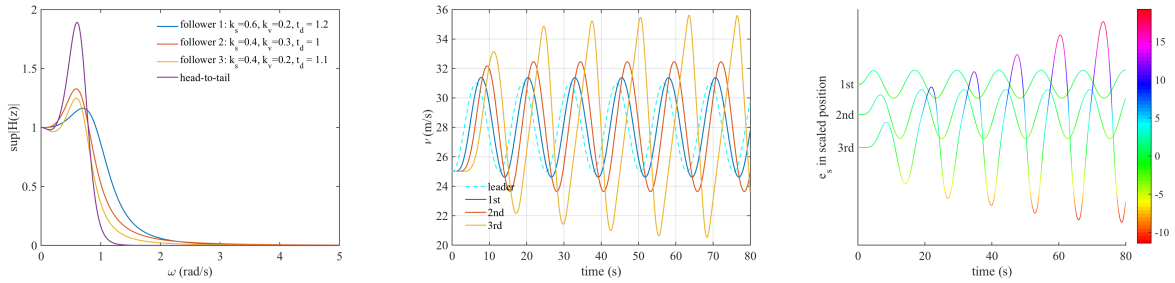

(a) analytical prediction (b) speed in time domain (c) gap error propagation with relative position of vehicles

Figure 7: Example 3: string instability of heterogeneous platoon under periodic leader disturbance

5 Infrastructure assisted adaptive driving strategy

At low market penetration rates, benefits of vehicle automation on traffic flow are limited (see Section 1) and the cooperation between automated vehicles and infrastructure (or traffic management) systems is needed to guarantee benefits on traffic [Hegyi et al., 2013, Wang et al., 2016a]. Adaptive driving strategies have been proposed to mitigate congestion at fixed bottlenecks with adaptive headways [Kesting et al., 2008]) based on heuristics. We propose a method to adaptively changing the parameters of one CAV in a platoon that can damp out speed disturbances and stabilise the platoon if unstable otherwise based on the analytical string stability conditions of heterogeneous strings derived from the previous section.

We make the following assumptions regarding the operations of the cooperative vehicle infrastructure system:

- The intelligent infrastructure system has a high-precision vehicle detection sub-system that gives detailed vehicle trajectories of the considered platoon in real time [Netten et al., 2013].
- With the high-precision sensing, the infrastructure system can estimate the parameters of non-connected ACC vehicles in the platoon [Monteil and Bouroche, 2016]. The estimation does not need to be perfect, as we will show in simulations with model mismatch in the ensuing.
- With trajectories of vehicles downstream of the considered platoon, the infrastructure can predict whether and when there is a disturbance in the speed profile of the platoon leader. This is a reasonable assumption, since typical highway disturbances of passing a shock wave or cutting-in of a merging vehicle near on-ramps are highly predictable with the high-precision sensing of the intelligent infrastructure system.
- One CAV that communicates its control and system parameters to the infrastructure stays in an arbitrary position in the platoon.
- The roadside system use the stability conditions derived from earlier sections to estimate whether the considered platoon is string stable. Based on *parsimonious control principle*, only when the string is estimated to be unstable, the infrastructure system computes the adaptive control parameters (e.g. desired time gap and feedback gains) for the CAV to suppress the predicted disturbance and stabilise the platoon, using the *stability margin* concept. The parameters are sent to the CAV via infrastructure-to-vehicle communication as *commanded parameters*.

- To prevent secondary disturbances to upstream traffic, the CAV smoothly changes its parameters (with linearly decaying rate) from the default value to the commanded values received from the infrastructure.
- At the end of the disturbance, the road infrastructure notifies the CAV to restore the default setting and the CAV uses the smooth transition strategy to restore the parameters to the default values.

The current concept and assumptions put the state estimation and prediction problem to the infrastructure side while focussing on the adaptive control design. Even more flexible is combining the adaptive control design with vehicle-based distributed traffic state prediction regimes, which is beyond the scope of this paper. Noteworthy is we only use one CAV in the derivation and simulations, but the proposed strategy is by no means restricted to that.

We remark that the parameter estimation for time-delayed systems is not trivial and should be treated rigorously in a separate work [Gomez et al., 2007]. In addition, this work aims at formulation of the adaptive strategy based on the string stability margin concept and demonstration of the concept in a few scenarios in simulation. Further challenges related to V2V based CAV controller design with time delay in real traffic should be addressed to continue this work [Ge and Orosz, 2017].

In the remainder of this section, we first present the methodology to determine the adaptive parameters of the CAV in the platoon, followed by verification of the effectiveness of the proposed method by simulation.

5.1 Adaptive driving parametrisation based on string stability conditions

The head-to-tail string stability definition and conditions for heterogeneous platoons allow us to manipulate the behaviour of CAVs in a platoon. Consider a general platoon of length k with one CAV positioned as nth vehicle in the platoon with $1 \leq n \leq k$. The rest autonomous vehicles that obtain information from and react to only the immediate predecessor.

From the string stability condition for heterogeneous platoon, we have the *head-to-tail* string stability condition as:

$$|\bar{H}_{1-k}(j\omega)| \leq |\mathcal{G}_{k,0}(\omega)| \prod_{j=1}^{k} |G_j(j\omega)| < 1, \forall \omega > 0 \tag{41}$$

with $\mathcal{G}_{k,0}(\omega) = \frac{1/G_k(j\omega) - 1 - j\omega \mathfrak{g}'_k(v_k)}{1/G_0(\omega) - 1 - j\omega \mathfrak{g}'_0(v_0)}$.

If the CAV is positioned within the string, e.g. $1 \leq n < k$, we cannot change the the magnitude of $\mathcal{G}_{k,0}(j\omega)$, but only $|G_n|$ with adaptive parametrisation. However, if the CAV is the tail of the string $n = k$, it is possible to change both $|G_k(j\omega)|$ and $|\mathcal{G}_{k,0}(j\omega)|$ to stabilise the mixed string. Intuitively, this means if the CAV is not the tail vehicle of the platoon, it has to work harder to stabilise the mixed string compared to the case when it is the tail vehicle. To this end, we derive the *stability margin* to choose the adaptive parameters of the CAV to stabilise the string based its position in the platoon:

- $1 \leq n < k$: If the CAV is the downstream of the platoon tail and the magnitude of the head-to-tail gap error transfer function is diverging, regulate parameters of the tail vehicle in such a way that the total magnitude of the head-to-tail gap error transfer function at different frequencies are below unity. Mathematically, this can be expressed as the following condition:

$$\max |G_n(\omega)| < \mathcal{M}^{\text{in}} \tag{42}$$

with the *stability margin for vehicle n within the k-length platoon* defined as:

$$\mathcal{M}^{\text{in}} = \frac{1}{\max \left[\mathcal{G}(\omega)_{k,0} \prod_{j=1, j\neq n}^{k} |G_j(\omega)| \right]} \tag{43}$$

- $n = k$: If the CAV is the tail of the platoon, the stabilising condition becomes:

$$\max \left[|\mathcal{G}(\omega)_{k,0}| \, |G_k(\omega)| \right] < \mathcal{M}^{\text{tail}} \tag{44}$$

with the *stability margin for the tail vehicle of the k-length platoon* defined as:

$$\mathcal{M}^{\text{tail}} = \frac{1}{\max \prod_{j=1}^{k-1} |G_j(\omega)|} \tag{45}$$

As we will show in Section 5.2, the adaptive driving strategy is more effective when the cooperative vehicle n is the tail of the platoon.

The finite length platoon setting allows us to define the head-to-tail string stability, which has practical implications in stabilising mixed traffic flow. Decomposing dense traffic into finite-length platoons allows us to derive the adaptive driving strategy for controlled vehicles in any finite-length platoon that attenuates the disturbance at the tail of the platoon. Repeating this throughout the whole traffic with randomly distributed controlled vehicles has the potential to prevent or delay traffic breakdown.

5.1.1 Smooth transition

The adaptive driving strategy entails changing control parameters of the cooperative vehicle and a resulting disturbance in the speed profile of the CAV. If the traffic density is high and the traffic stream following the cooperative vehicle is unstable, this can create a secondary disturbance propagation while suppressing the first one. To this end, we implement a smooth transition strategy between two parameter sets: default set $\mathcal{K}_d$ and the adaptive set $\mathcal{K}^{(a)}$. Within a transition time T, we impose the linear change from the default parameter to the adaptive one as:

$$\mathcal{K}(t) = \mathcal{K}^{(d)} + \frac{(\mathcal{K}^a - \mathcal{K}^d)(t - t^s)}{T} \text{ if } t \in [t^s, t^s + T] \tag{46}$$

where t^s denotes the start of the transition. $\mathcal{K}$ can be specified as t_d, k_s and k_v when applicable. Similar procedure is implemented for the transition from the adaptive parameters to the default parameters.

It should be noted that changing the feedback gains will not alter the equilibrium state of the ACC controller and previous work suggested that it may not be necessary to use the transition algorithm [Han et al., 2015]. However, changing the desired time leads to jump in equilibrium state and the transition algorithm is effective in smoothing jerky behaviour in the transient process. The transient law has the benefit of keeping the ACC controller input within admissible bounds.

5.2 Simulation verification

This section demonstrates the effectiveness of the adaptive driving strategy when the infrastructure system has perfect knowledge of the platoon behaviour and when the platoon behaviour model is imperfect respectively.

5.2.1 Simulation with perfect model

In the first case, we consider a platoon of 5 ACC followers employing the linear CTG policy, one of which is a CAV. The default ACC parameters are: $k_s = 0.4, k_v = 0.2, t_d = 1.2, \xi = 0.2, \tau = 0.2$. The analytical string stability condition suggests that the homogeneous string is not stable, see the green line in Figure 8(a). The adaptive driving strategy is to change the desired time gap from 1.2 s to 3 s before passing the disturbance, which results in the maximum magnitude of the error transfer function less than unity when the CAV vehicle is the platoon tail, see the dashed line in Figure 8(a). Although the total magnitude of the whole platoon when the CAV is not the platoon tail is larger than 1, which does not guarantee string stability, it is much lower than the case without adaptive driving (blue line in Figure 8(a)).

To test the performance of the adaptive driving strategy, we simulate a platoon of 6 vehicles with an exogenous leader, using the same leader speed profile as in Figure 4. To show the robustness of the approach, we vary the position of the adaptive vehicle in the platoon to be the 3rd, 4th and 5th (tail) follower in the platoon. The results are shown in Figure 8. Compared to the case without adaptive driving strategy, the gap error at the platoon tail under the adaptive driving strategy is much smaller in amplitude. It is also observed that the effects of the cooperative driving is less significant when the position of the cooperative vehicle moves forward in the platoon and the effect is most pronounced when the cooperative vehicle is the platoon tail. Nevertheless, the benefits in suppressing the amplification of the disturbance hold with varying positions of the cooperative vehicle in the platoon.

As predicted by the analytical solution, an adaptive time gap of 3 s only guarantees string stability when the CAV is the platoon tail. When the CAV is not the platoon tail, it has to work harder to ensure string stability. With the guidance of the string stability margin (42), we are able to stabilise the platoon with a larger desired time gap of 4.8 s, as shown in Figure 9(a). The resulting gap propagation and gap error profiles when the 3rd vehicle is the CAV are shown in Figure 9(b),9(c). The effects in damping out the disturbance are more pronounced when comparing the tail vehicle gap error between 30 seconds and 60 seconds of the simulation in Figure 8(m) and 9(c).

As we discussed earlier, the transition law smooths the response due to a jump in the steady state if the desired time gap is changed. The transition time T influences the amplitude of the response of the adaptive vehicle due to jump in desired time gap. The larger T is, the smoother the resulting accelerations of the adaptive

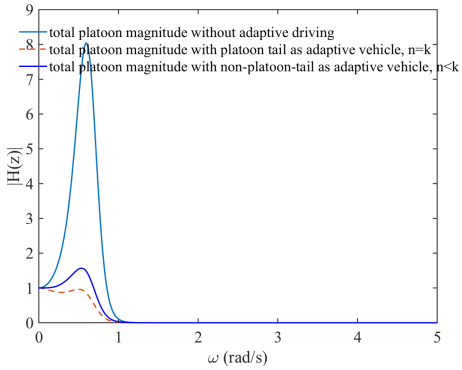

(a) Analytical solution

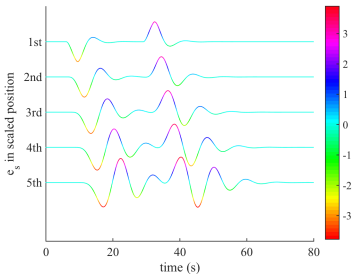

(b) Without adaptive driving: gap error propgation

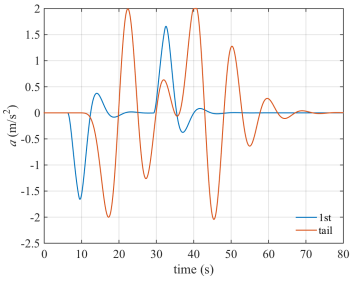

(c) Without adaptive driving: acceleration

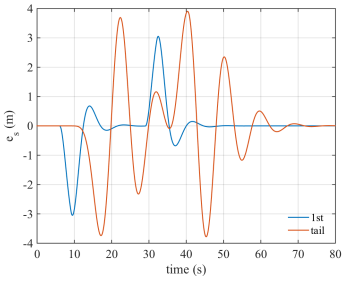

(d) Without adaptive driving: gap error propgation

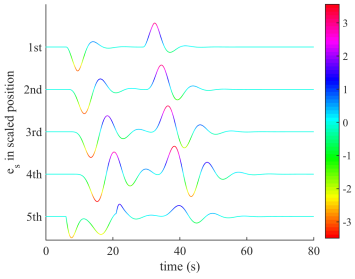

(e) 5th follower adaptive: gap error propagation

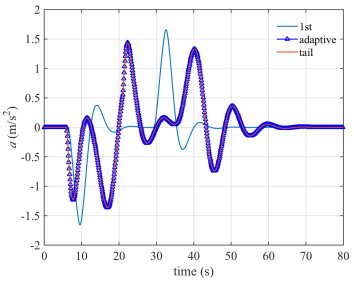

(f) 5th follower adaptive: acceleration

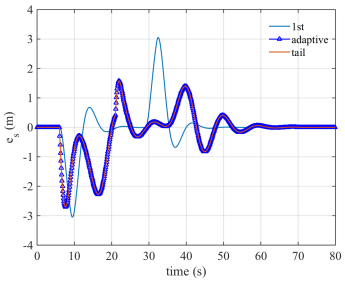

(g) 5th follower adaptive: gap error

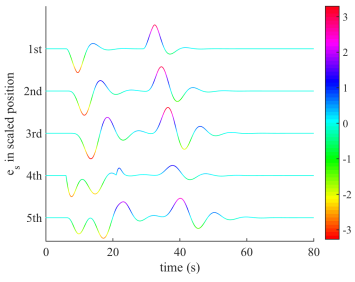

(h) 4th follower adaptive: gap error propagation

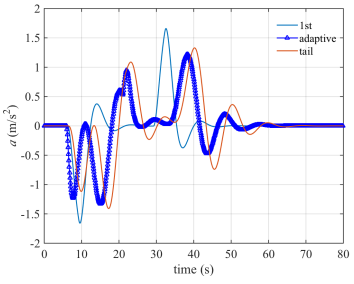

(i) 4th follower adaptive: acceleration

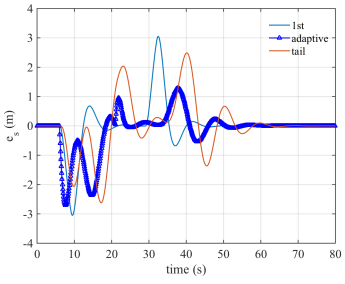

(j) 4th follower adaptive: gap error

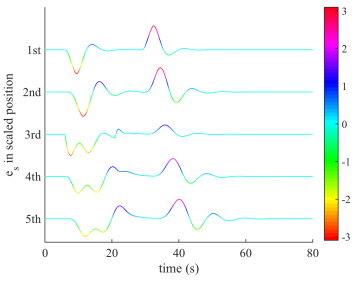

(k) 3rd follower adaptive: gap error propagation

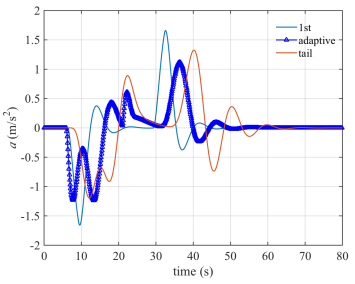

(l) 3rd follower adaptive: acceleration

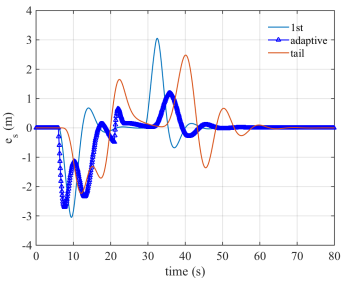

(m) 3rd follower adaptive: gap error

Figure 8: Analytical prediction of the mixed platoon stability and verification of adaptive driving strategy

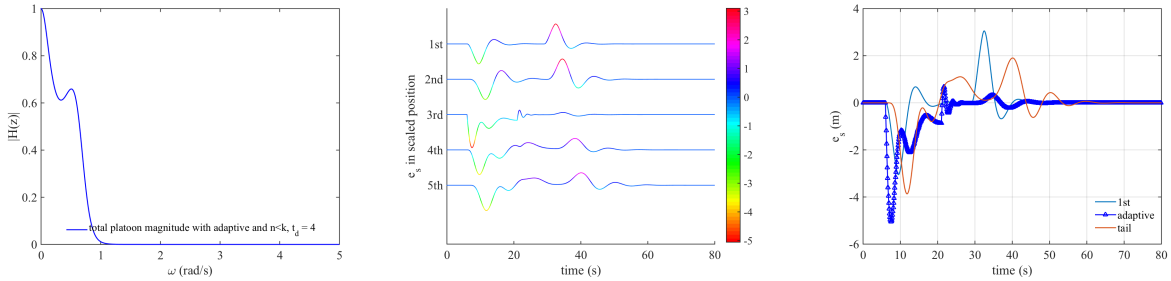

(a) analytical prediction

(b) 3rd follower adaptive: gap error propagation

(c) 3rd follower adaptive: gap error

Figure 9: 3rd follower as adaptive vehicle with a larger adaptive time gap of $t_d^{(a)} = 4.8$ s. Other parameters are the same.

vehicle with the new desired time gap. In the simulation experiments, we choose T as 15 s. A sensitivity analysis in Appendix C shows need for the smooth transition.

5.2.2 Simulation with model mismatch

The simulation results shown in Figure 8 is based on the perfect model, i.e. there is no mismatch between the vehicle dynamics and control laws of vehicles between analytical prediction and simulation. Intuitively, this requires the infrastructure to perfectly estimate the vehicle system dynamics and control parameters of the non-connected ACC vehicles. In reality, the estimation of the non-connected ACC behavioural models is deemed imperfect due to measurement errors and uncertainties in vehicle dynamics. To demonstrate the robustness of the proposed approach, we conduct more simulations under model mismatch.

We model two categories of model mismatch in this paper: one related to the vehicle system dynamics and the other related to the control parameters. In the vehicle dynamics model (2), τ reflects the retarded time between the control command u and the actual vehicle acceleration a and is considered as constant previously. In reality, the actuation lag is influenced by vehicle speeds, road gradients, road surface conditions and is thus difficult to be estimated perfectly. Therefore, we assume that the actuator lag is stochastic and evenly distributed in the range of $[0.5\tau, 1.5\tau]$ s in the simulation, while using the constant $\tau = 0.2$ s in analytical derivations. For the control parameters, the desired time gap is relatively easy to estimate since this is the equilibrium gap a vehicle maintains. The feedback gains are more difficult for the infrastructure system to estimate. Therefore, we model two types of errors of the feedback gains (k_s and k_d), overestimate and underestimate at a relative error of 10%. That is, for the overestimate scenario, we use $k_s' = (1 + 10\%)k_s, k_d' = (1 + 10\%)k_d$ for the simulation of non-connected ACC vehicles, while using k_d, k_s in the analytical prediction. The simulation results under the same leader speed profile scenario with the platoon tail as the CAV are shown in Figure 10(a-d) with adaptive gap of 3 s. Gap error propagation plots clearly show that although errors are included vehicle dynamics and control parameters, the adaptive driving strategy still suppresses the disturbance effectively.

In reality, the actuator lag can be as large as 0.5 s. We test the proposed algorithm with a larger match of actuator lag: i.e. we still use $\tau = 0.2$ s in the analytical derivation, but simulate the vehicle motions with actuator lag varying stochastically between $[0.2, 0.6]$ s and 10% underestimate of the feedback gains. The gap error propagation plots are shown in Figure 10(e) and (f). The results further verify the effectiveness of the proposed strategy.

While the proposed strategy can be beneficial for traffic and works at low market penetration rate, it should be noted that the lower the market penetration rate, the harder the controlled vehicles have to work to suppress disturbance in the platoon.

6 Conclusion and future work

We proposed an approach to adaptively regulating the parameters of control systems for CAV in a platoon to stabilise downstream speed disturbances based on *vehicle-infrastructure cooperation concepts*. The approach is based on string stability analysis of heterogeneous vehicle strings in frequency domain. The analytical string stability conditions give new insights into the relationship between the string stability properties of mixed strings, the system properties of time delays and controller design parameters of feedback gains and desired time gap. It provides rigorous guidance in designing control parameters of cooperative vehicles based on parsimonious control principle to suppress disturbance propagation.

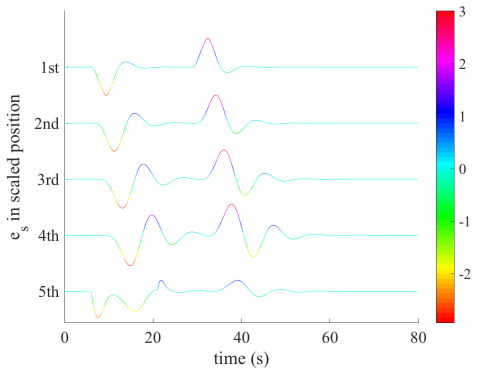

(a) gap error propagataion 10% overestimate of feedback gains and stochastic actuator lag between 0.1 and 0.3 s

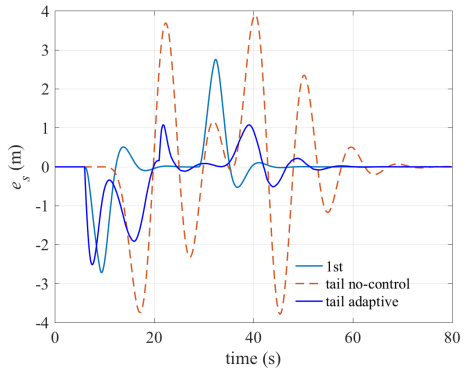

(b) gap error with 10% overestimate of feedback gains and stochastic actuator lag between 0.1 and 0.3 s

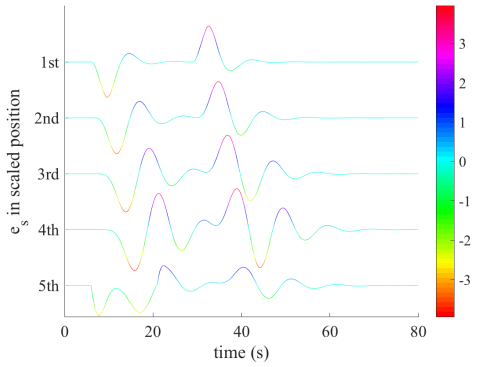

(c) gap error propagataion 10% underestimate of feedback gains and stochastic actuator lag between 0.1 and 0.3 s

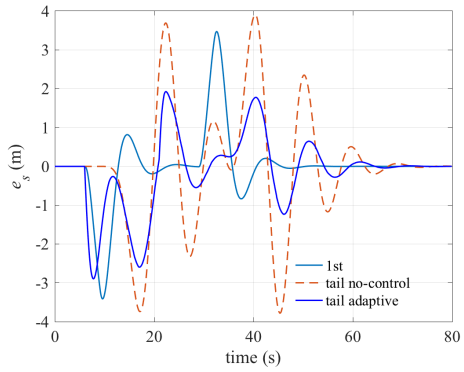

(d) gap error with 10% underestimate of feedback gains and stochastic actuator lag between 0.1 and 0.3 s

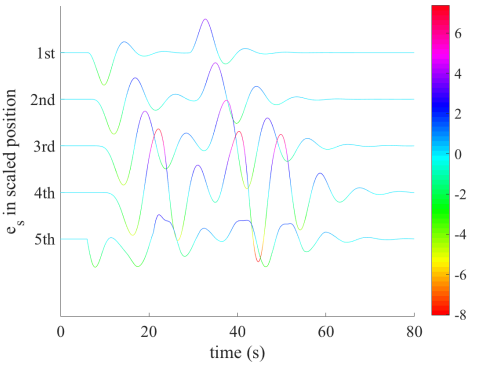

(e) gap error propagataion with 10% underestimate of feedback gains and stochastic actuator lag between 0.2 and 0.6 s

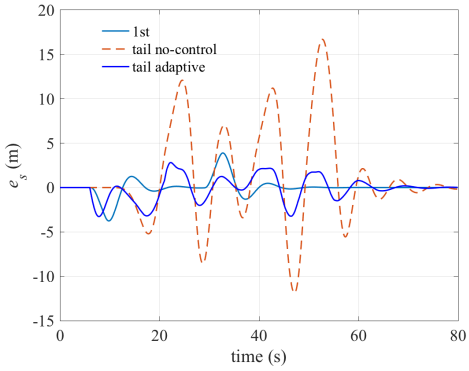

(f) gap error with 10% underestimate of feedback gains and stochastic actuator lag between 0.2 and 0.6 s

Figure 10: Simulation verification under model mismatch with follower 5 (tail vehicle) as the cooperative vehicle and adaptive time gap of 3 s. Red dashed lines show the gap errors of tail vehicle in the reference case without adaptive control.

Analytical results are verified via systematic simulation of both homogeneous and heterogeneous strings. Simulations demonstrate the predictive power of the analytical string stability conditions and the benefits of the adaptive driving strategy. The adaptive driving strategy appears to be robust against model mismatch and order of the platoon.

This work entails two-step communication of V2I and I2V, which may add problems in communication. The V2I and I2V communication channel is not modelled explicitly and the model mismatch remains at the parametric level. These are the points of attention for next-step studies. We should also acknowledge that the vehicle behaviour in simulation is a simplification of reality and further tests with more realistic vehicle dynamics model are needed to prove the effectiveness of the proposed strategy. Another question to investigate further is whether a change in desired time gap can guarantee string stability without the transition algorithm. Future research is also directed to integrate V2V communication topology and adaptive control design for stable platooning systems.

Acknowledgement

The author would like to thank the anonymous reviewers for their valuable comments on this article.

References

[Ge and Orosz, 2014] Ge, J. I. and Orosz, G. (2014). Dynamics of connected vehicle systems with delayed acceleration feedback. *Transportation Research Part C: Emerging Technologies*, 46(0):46 – 64.

[Ge and Orosz, 2017] Ge, J. I. and Orosz, G. (2017). Optimal control of connected vehicle systems with communication delay and driver reaction time. *IEEE Transactions on Intelligent Transportation Systems*, 18(8):2056–2070.

[Gomez et al., 2007] Gomez, O., Orlov, Y., and Kolmanovsky, I. V. (2007). On-line identification of siso linear time-invariant delay systems from output measurements. *Automatica*, 43(12):2060 – 2069.

[Han et al., 2015] Han, D., Mo, Y., and Murray, R. M. (2015). Synthesis of distributed longitudinal control protocols for a platoon of autonomous vehicles. In *Proceedings of the 54th IEEE Conference on Decision and Control*.

[Hegyi et al., 2013] Hegyi, A., Netten, B., Wang, M., Schakel, W., Schreiter, T., Yuan, Y., van Arem, B., and Alkim, T. (2013). A cooperative systems based variable speed limit control algorithm against jam waves - an extension of the SPECIALIST algorithm. In *16th International IEEE Conference on Intelligent Transportation Systems*, pages 973–978, The Hague, The Netherlands.

[Jia and Ngoduy, 2016] Jia, D. and Ngoduy, D. (2016). Platoon based cooperative driving model with consideration of realistic inter-vehicle communication. *Transportation Research Part C: Emerging Technologies*, 68:245 – 264.

[Kesting et al., 2008] Kesting, A., Treiber, M., Schonhof, M., and Helbing, D. (2008). Adaptive cruise control design for active congestion avoidance. *Transportation Research Part C: Emerging Technologies*, 16(6):668–683.

[Milanés and Shladover, 2014] Milanés, V. and Shladover, S. E. (2014). Modeling cooperative and autonomous adaptive cruise control dynamic responses using experimental data. *Transportation Research Part C: Emerging Technologies*, 48(0):285 – 300.

[Monteil et al., 2014] Monteil, J., Billot, R., Sau, J., and El Faouzi, N.-E. (2014). Linear and weakly nonlinear stability analyses of cooperative car-following models. *Intelligent Transportation Systems, IEEE Transactions on*, 15(5):2001–2013.

[Monteil and Bouroche, 2016] Monteil, J. and Bouroche, M. (2016). Robust parameter estimation of car-following models considering practical non-identifiability. In *2016 IEEE 19th International Conference on Intelligent Transportation Systems (ITSC)*, pages 581–588.

[Mullakkal-Babu et al., 2016] Mullakkal-Babu, F. A., Wang, M., Van Arem, B., and Happee, R. (2016). Design and analysis of full range adaptive cruise control with integrated collision avoidance strategy. In *19th International IEEE Conference on Intelligent Transportation Systems*, Rio de Janerio, Brazil.

[Naus et al., 2010] Naus, G., Vugts, R., Ploeg, J., van de Molengraft, M., and Steinbuch, M. (2010). String-stable cacc design and experimental validation: A frequency-domain approach. *Vehicular Technology, IEEE Transactions on*, 59(9):4268 –4279.

[Netten et al., 2013] Netten, B., Hegyi, A., Wang, M., Schakel, W., Yuan, Y., Schreiter, T., van Arem, B., van Leeuwen, C., and Alkim, T. (2013). Improving moving jam detection performance with v2i communication. In *20th World Congress on Intelligent Transport Systems*, Tokyo, Japan.

[Ngoduy, 2015] Ngoduy, D. (2015). Effect of the car-following combinations on the instability of heterogeneous traffic flow. *Transportmetrica B: Transport Dynamics*, 3(1):44–58.

[Ploeg et al., 2014] Ploeg, J., van de Wouw, N., and Nijmeijer, H. (2014). L_p string stability of cascaded systems: Application to vehicle platooning. *IEEE Transactions on Control Systems Technology*, 22(2):786–793.

[Sheikholeslam and Desoer, 1993] Sheikholeslam, S. and Desoer, C. (1993). Longitudinal control of a platoon of vehicles with no communication of lead vehicle information: a system level study. *Vehicular Technology, IEEE Transactions on*, 42(4):546–554.

[Shladover et al., 2015] Shladover, S. E., Nowakowski, C., Lu, X.-Y., and Ferlis, R. (2015). Cooperative adaptive cruise control. *Transportation Research Record: Journal of the Transportation Research Board*, 2489:145–152.

[Shladover et al., 2012] Shladover, S. E., Su, D., and Lu, X.-Y. (2012). Impacts of cooperative adaptive cruise control on freeway traffic flow. *Transportation Research Record: Journal of the Transportation Research Board*, 2324:63–70.

[Talebpour and Mahmassani, 2016] Talebpour, A. and Mahmassani, H. S. (2016). Influence of connected and autonomous vehicles on traffic flow stability and throughput. *Transportation Research Part C: Emerging Technologies*, 71:143 – 163.

[Treiber and Kesting, 2011] Treiber, M. and Kesting, A. (2011). Evidence of convective instability in congested traffic flow: A systematic empirical and theoretical investigation. *Transportation Research Part B: Methodological*, 45(9):1362–1377.

[Treiber and Kesting, 2013] Treiber, M. and Kesting, A. (2013). *Traffic Flow Dynamics - Data, Models and Simulation*. Springer.

[Treiber et al., 2006] Treiber, M., Kesting, A., and Helbing, D. (2006). Delays, inaccuracies and anticipation in microscopic traffic models. *Physica A: Statistical Mechanics and its Applications*, 360(1):71–88.

[Van Arem et al., 2006] Van Arem, B., van Driel, C. J. G., and Visser, R. (2006). The impact of cooperative adaptive cruise control on traffic-flow characteristics. *IEEE Transactions on Intelligent Transportation Systems*, 7(4):429–436.

[VanderWerf et al., 2001] VanderWerf, J., Shladover, S. E., Kourjanskaia, N., Miller, M., and Krishnan, H. (2001). Modeling effects of driver control assistance systems on traffic. *Transportation Research Record: Journal of the Transportation Research Board*, 1748:167–174.

[Varaiya and Shladover, 1991] Varaiya, P. and Shladover, S. E. (1991). Sketch of an IVHS systems architecture. In *Vehicle Navigation and Information Systems Conference*, volume 2, pages 909–922.

[Wang et al., 2014a] Wang, M., Daamen, W., Hoogendoorn, S. P., and van Arem, B. (2014a). Rolling horizon control framework for driver assistance systems. Part I: Mathematical formulation and non-cooperative systems. *Transportation Research Part C: Emerging Technologies*, 40:271–289.

[Wang et al., 2014b] Wang, M., Daamen, W., Hoogendoorn, S. P., and van Arem, B. (2014b). Rolling horizon control framework for driver assistance systems. Part II: Cooperative sensing and cooperative control. *Transportation Research Part C: Emerging Technologies*, 40:290–311.

[Wang et al., 2016a] Wang, M., Daamen, W., Hoogendoorn, S. P., and van Arem, B. (2016a). Connected variable speed limits control and car-following control with vehicle-infrastructure communication to resolve stop-and-go waves. *Journal of Intelligent Transportation Systems*.

[Wang et al., 2016b] Wang, M., Daamen, W., Hoogendoorn, S. P., and van Arem, B. (2016b). Cooperative car-following control: Distributed algorithm and impact on moving jam features. *IEEE Transactions on Intelligent Transportation Systems*, 17(5):1459–1471.

[Wang et al., 2015] Wang, M., Hoogendoorn, S. P., Daamen, W., van Arem, B., and Happee, R. (2015). Game theoretic approach for predictive lane-changing and car-following control. *Transportation Research Part C: Emerging Technologies*, 58:73 – 92.

[Wang et al., 2016c] Wang, M., Hoogendoorn, S. P., Daamen, W., van Arem, B., Shyrokau, B., and Happee, R. (2016c). Delay-compensating strategy to enhance string stability of adaptive cruise controlled vehicles. *Transportmetrica B: Transport Dynamics*, 0(0):1–19.

[Wang et al., 2017] Wang, M., Li, H., Gao, J., Huang, Z., Li, B., and van Arem, B. (2017). String stability of heterogeneous platoons with non-connected automated vehicles. In *2017 IEEE 20th International Conference on Intelligent Transportation Systems (ITSC)*, pages 1–8.

[Wilson, 2008] Wilson, R. E. (2008). Mechanisms for spatio-temporal pattern formation in highway traffic models. *Philosophical Transactions of the Royal Society A: Mathematical, Physical and Engineering Sciences*, 366(1872):2017–2032.

[Xiao and Gao, 2011] Xiao, L. and Gao, F. (2011). Practical string stability of platoon of adaptive cruise control vehicles. *Intelligent Transportation Systems, IEEE Transactions on*, 12(4):1184–1194.

[Xiao et al., 2017] Xiao, L., Wang, M., and van Arem, B. (2017). Realistic car-following models for microscopic simulation of adaptive and cooperative adaptive cruise control vehicles. *Transportation Research Record: Journal of the Transportation Research Board*.

[Zhang and Orosz, 2016] Zhang, L. and Orosz, G. (2016). Motif-based design for connected vehicle systems in presence of heterogeneous connectivity structures and time delays. *IEEE Transactions on Intelligent Transportation Systems*, 17(6):1638–1651.

[Zhou et al., 2017] Zhou, F., Li, X., and Ma, J. (2017). Parsimonious shooting heuristic for trajectory design of connected automated traffic part i: Theoretical analysis with generalized time geography. *Transportation Research Part B: Methodological*, 95:394 – 420.

[Zhou and Peng, 2005] Zhou, J. and Peng, H. (2005). Range policy of adaptive cruise control vehicles for improved flow stability and string stability. *IEEE Transactions on Intelligent Transportation Systems*, 6(2):229–237.

Appendix A: Exact linearisation of longitudinal dynamics

Here we show the linearisation of the longitudinal vehicle dynamics. In Eq. (1), the aerodynamic drag is a nonlinear function of velocity:

$$R_{a,i} = K_{d,i}\dot{x}_i^2 \text{ with } K_{d,i} = \frac{\rho A_i C_{d,i}}{2} \tag{47}$$

where $K_{d,i}$ denotes the aerodynamic drag coefficient, ρ denotes the specific mass of air. A_i is the cross-sectional area of vehicle i and $C_{d,i}$ denotes i-th vehicle's drag coefficient. $R_{d,i}$ denotes vehicle's mechanical drag.

The engine dynamics is modelled with a first-order time lag:

$$\dot{F}_i = -\frac{F_i}{\tau_i} + \frac{U_i}{\tau_i} \tag{48}$$

U_i denotes the command input to vehicle's engine (via the throttle). τ_i denotes the vehicle's engine time-constant.

A so-called exact linearisation method is used to derive a linear model for vehicles driving on flat roads, i.e. $R_{g,i} = 0$ [Sheikholeslam and Desoer, 1993, Xiao and Gao, 2011]. Substituting F_i in the right hand side of Eq. (48) with Eq. (1) we get:

$$\dot{F}_i = -\frac{m_i\ddot{x}_i + K_{d,i}\dot{x}_i^2 + R_{d,i}}{\tau_i} + \frac{U_i}{\tau_i} \tag{49}$$

Differentiating both sides of Eq. (1) with respect to time and inserting Eq. (49) arrives at:

$$\dddot{x}_i = -\frac{m_i\ddot{x}_i + K_{d,i}\dot{x}_i^2 + R_{d,i}}{m_i\tau_i} - \frac{2K_{d,i}\dot{x}_i\ddot{x}_i}{m_i} + \frac{U_i}{m_i\tau_i} \tag{50}$$

$$\dddot{x}_i = -\frac{\ddot{x}_i}{\tau_i} - \frac{K_{d,i}\dot{x}_i^2 + R_{d,i}}{m_i\tau_i} - \frac{2K_{d,i}\dot{x}_i\ddot{x}_i}{m_i} + \frac{U_i}{m_i\tau_i} \tag{51}$$

We choose the following nonlinear state feedback control law for the lower-level control system:

$$U_i = K_{d,i}\dot{x}_i^2 + R_{d,i} + 2K_{d,i}\dot{x}_i\ddot{x}_i\tau_i + m_i u_i \tag{52}$$

Here we introduce a new control input u_i, which can be interpreted as the *desired acceleration* of the controlled vehicle i. Inserting (52) to (51) and write the full vector we get the linear differential equation (2). The nonlinear control law at the lower level linearises the vehicle dynamics and results in a model that is independent of vehicle's particular characteristics (e.g., mass, aerodynamic drag coefficient, etc.), while keeping the characteristics of the driveline dynamics (at the linear level) [Sheikholeslam and Desoer, 1993, Xiao and Gao, 2011].

Appendix B: Proof of Theorem 3.4

For homogeneous strings with delays, the the speed transfer function 11 can rewritten as:

$$\begin{aligned} G(z) &= \frac{(f_{v_p}z + f_s)e^{-\xi z}}{\tau z^3 + z^2 - f_v e^{-\xi z}z + f_s e^{-\xi z}} \cdot \frac{e^{\xi z}}{e^{\xi z}} \\ &= \frac{(f_{v_p}z + f_s)}{\tau z^3 e^{\xi z} + z^2 e^{\xi z} - f_v z + f_s} = \frac{UP}{LP} \end{aligned} \tag{53}$$

Inserting $z = j\omega$ into the upper part of the aforementioned equation and take the 2-norm:

$$UP = j\omega f_{v_p} + f_s \tag{54}$$

$$|UP| = \omega^2 f_{v_p}^2 + f_s^2 \tag{55}$$

Inserting $z = j\omega$ into the lower part of the aforementioned equation and note:

$$e^{\xi z} = e^{\xi j\omega} = \cos(\xi\omega) + j\sin(\xi\omega) \tag{56}$$

$$LP = \underbrace{\tau z^3 e^{\xi z}}_{(1)} + \underbrace{z^2 e^{\xi z}}_{(2)} \underbrace{-f_v z}_{(3)} + \underbrace{f_s}_{(4)} \tag{57}$$

$$\begin{aligned} (1) &= \tau(j\omega)^3 e^{\xi j\omega} = -\tau j\omega^3(\cos(\xi\omega) + j\sin(\xi\omega)) && (58)\\ (2) &= (j\omega)^2 e^{\xi j\omega} = -\omega^2(\cos(\xi\omega) + j\sin(\xi\omega)) && (59)\\ (3) &= -f_v j\omega && (60)\\ (4) &= f_s && (61) \end{aligned}$$

$$\begin{aligned} (1)+(2)+(3)+(4) &= -\tau j\omega^3(\cos(\xi\omega) + j\sin(\xi\omega)) - \omega^2\cos(\xi\omega) + j\sin(\xi\omega) - f_v j\omega + f_s \\ &= \tau\omega^3\sin(\xi\omega) - \omega^2\cos(\xi\omega) + f_s - j\left(\tau\omega^3\cos(\xi\omega) + \omega^2\sin(\xi\omega) + f_v\omega\right) \\ &= \underbrace{\omega^2(\tau\omega\sin(\xi\omega) - \cos(\xi\omega)) + f_s}_{(5)} - \underbrace{j\left(\omega^2(\tau\omega\cos(\xi\omega) + \sin(\xi\omega)) + f_v\omega\right)}_{(6)} \end{aligned} \tag{62}$$

Thus the 2-norm of the lower part:

$$|(1)+(2)+(3)+(4)| = (5)^2 + (6)^2 \tag{63}$$

and

$$\begin{aligned} (5)^2 &= \omega^4(\tau\omega\sin(\xi\omega) - \cos(\xi\omega))^2 + f_s^2 + 2\omega^2 f_s(\tau\omega\sin(\xi\omega) - \cos(\xi\omega)) \\ &= \omega^4(\tau^2\omega^2\sin^2(\xi\omega) - 2\tau\omega\sin(\xi\omega)\cos(\xi\omega) + \cos^2(\xi\omega)) + f_s^2 + 2\omega^2 f_s(\tau\omega\sin(\xi\omega) - \cos(\xi\omega)) \\ &= \sin^2(\xi\omega)\omega^6 - 2\tau\sin(\xi\omega)\cos(\xi\omega)\omega^5 + \cos^2(\xi\omega)\omega^4 + 2f_s\tau\sin(\xi\omega)\omega^3 - 2f_s\cos(\xi\omega)\omega^2 + f_s^2 \end{aligned} \tag{64}$$

$$\begin{aligned} (6)^2 &= \omega^4(\tau\omega\cos(\xi\omega) + \sin(\xi\omega))^2 + f_v^2\omega^2 + 2\omega^2(\tau\omega\cos(\xi\omega) + \sin(\xi\omega))f_v\omega \\ &= \tau^2\cos^2(\xi\omega)\omega^6 + 2\tau\sin(\xi\omega)\cos(\xi\omega)\omega^5 + \sin^2(\xi\omega)\omega^4 + f_v^2\omega^2 \\ &\quad + 2f_v\tau\cos(\xi\omega)\omega^4 + 2f_v\sin(\xi\omega)\omega^3 \end{aligned} \tag{65}$$

$$(5)^2 + (6)^2 = \tau^2\omega^6 + (1 + 2f_v\tau\cos(\xi\omega))\omega^4 + 2(f_s\tau + f_v)\sin(\xi\omega)\omega^3 + (-2f_s\cos(\xi\omega) + f_v^2)\omega^2 + f_s^2 \tag{66}$$

String stability requires $\left|\frac{UP}{LP}\right| \leq 1$,
Specifying the two parts leads to:

$$\frac{f_{v_p}^2\omega^2 + f_s^2}{\tau^2\omega^6 + (1 + 2f_v\tau\cos(\xi\omega))\omega^4 + 2(f_s\tau + f_v)\sin(\xi\omega)\omega^3 + (-2f_s\cos(\xi\omega) + f_v^2)\omega^2 + f_s^2} \leq 1 \tag{67}$$

One assumption here is $f_v + f_s\tau < 0$. Note that this is not very restrictive since the partial derivatives along the equilibrium are not independent [Treiber and Kesting, 2013] and follows:

$$f_s\mathfrak{g}'(v) + f_v + f_{v_p} = 0 \tag{68}$$

As $f_{v_p} \geq 0$, this gives:

$$f_v + f_s\mathfrak{g}'(v) \leq 0 \tag{69}$$

the only assumption is that *the desired time gap* $\mathfrak{g}'(v)$ *is larger than the actuator delay.* This is a quite plausible assumption.

$$\mathfrak{g}'(v) > \tau \tag{70}$$

This gives:

$$f_v + f_s\tau < f_v + f_s\mathfrak{g}'(v) \leq 0 \tag{71}$$

Note that $\sin(\xi\omega) \leq \xi\omega$ for $\xi \geq 0$ and $\omega > 0$, $\cos(\xi\omega) \leq 1$, $f_v < 0$ and $f_v + f_s\tau < 0$ thus condition 67 becomes:

$$\begin{aligned}
&\frac{f_{v_p}^2\omega^2 + f_s^2}{\tau^2\omega^6 + (1 + 2f_v\tau\cos(\xi\omega))\omega^4 + 2(f_s\tau + f_v)\sin(\xi\omega)\omega^3 + (-2f_s\cos(\xi\omega) + f_v^2)\omega^2 + f_s^2} \\
&\leq \frac{f_{v_p}^2\omega^2 + f_s^2}{\tau^2\omega^6 + (1 + 2f_v\tau)\omega^4 + 2(f_s\tau + f_v)\xi\omega\omega^3 + (-2f_s + f_v^2)\omega^2 + f_s^2} \\
&= \frac{f_{v_p}^2\omega^2 + f_s^2}{\tau^2\omega^6 + (1 + 2f_v\tau + 2f_s\tau\xi + 2f_v\xi)\omega^4 + (-2f_s + f_v^2)\omega^2 + f_s^2} \leq 1
\end{aligned} \tag{72}$$

which simplifies as:

$$|G(z)| \leq \frac{f_{v_p}^2\omega^2 + f_s^2}{\tau^2\omega^6 + (1 + 2f_v\tau + 2f_s\tau\xi + 2f_v\xi)\omega^4 + (-2f_s + f_v^2)\omega^2 + f_s^2} \leq 1 \tag{73}$$

Q.E.D.

Appendix C: Sensitivity of transition time T

Here we conducted simulation experiments with the same setting except a different transition time T as the experiment in Figure 8 with the tail vehicle as the adaptive vehicle. The resulting accelerations of the adaptive vehicles are shown in Figure 11, with $T = 0, 5, 10, 15$ respectively.

It can be seen clearly that without the transient algorithm ($T = 0$), the adaptive vehicle accelerations are saturated at the lower bound of $a_{min} = -4$ m/s^2. This is undesired as it is outside the design domain of ACC controller. With $T = 5, 10, 15$ s, the resulting accelerations of the adaptive vehicle are much smoother.

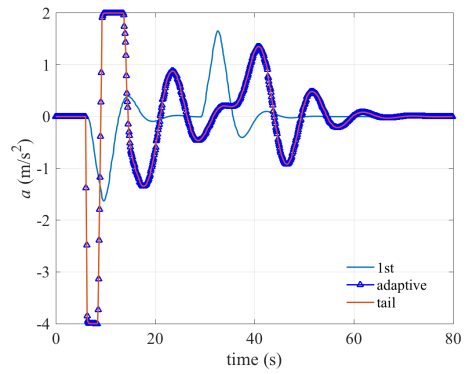

(a) Without smooth transition

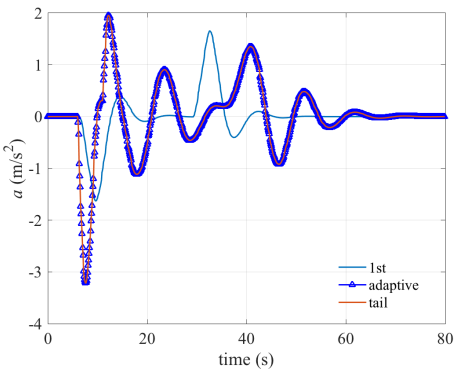

(b) Transition time 5 s

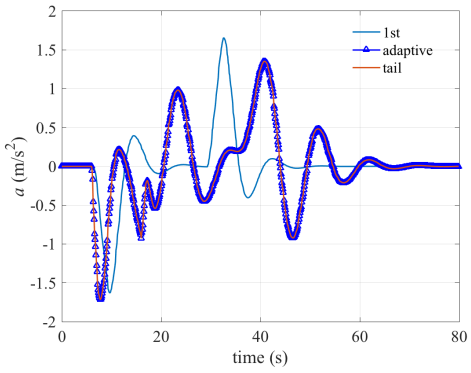

(c) Transition time 10 s

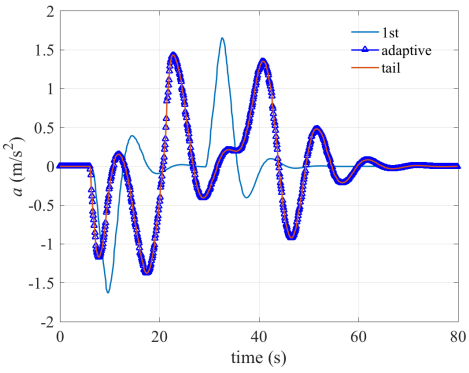

(d) Transition time 15 s

Figure 11: 5th follower as adaptive vehicle with a larger adaptive time gap of $t_d^{(a)} = 3$ s under different transition time T. Other parameters are the same as in Figure 8(f).